

Observational Viability of Anisotropic Inflation Revisited

Maryam Roushan ¹, Narges Rashidi ², Kourosh Nozari ³

Department of Theoretical Physics, Faculty of Science, University of Mazandaran,
P. O. Box 47416-95447, Babolsar, IRAN

Abstract

We investigate anisotropic inflation within the single-field model featuring an intermediate scale factor. Our analysis reveals that the anisotropic nature of the Friedmann equations in this framework affects the slow-roll parameters, which in turn influence key perturbation parameters. Using a numerical approach, we derive constraints on the intermediate parameter β and the anisotropic parameter c . Our results show that the model is consistent with Planck2018 TT, TE, EE +lowE+lensing+BK14+BAO data at 68% CL, for $0.84 < \beta < 1$ and $7.34 < c < 27.7$. At 95% CL the consistency holds for $0.77 < \beta < 1$ and $7.17 < c < 28.9$. The model is also consistent with Planck2018 TT, TE, EE +lowE+lensing+BK18+BAO data, for $0.91 < \beta < 1$ and $8.00 < c < 27.4$ (at 68% CL), and $0.88 < \beta < 1$ and $7.40 < c < 28.8$ (at 95% CL). Additionally, we examine the reheating phase using these constraints on constraints on β and c and determine the observationally consistent ranges for the number of e-folds and the temperature during the reheating phase.

Key Words: Intermediate Anisotropic Inflation; Reheating; Observational Viability.

¹m.roushan@umz.ac.ir

²n.rashidi@umz.ac.ir (Corresponding Author)

³knozari@umz.ac.ir

1 Introduction

To address some important shortcomings of the standard model of cosmology, the intriguing inflationary paradigm has been proposed [1]. This framework offers an elegant explanation for the dynamics of the universe during its earliest moments. In Ref. [2], the author presents a new inflationary model that resolves the issues of the old inflation model. In Ref. [3], it was proposed that a more detailed examination of first-order phase transitions in GUT models could help resolve some of the biggest puzzles in cosmology. Observational tests of cosmic inflation and the possibility of reconstructing the inflaton potential based on data were examined in Ref. [4]. More significantly, inflation provides an explanation for how the large-scale structure of the universe was initially seeded. The simplest inflationary models rely on the slow-roll conditions, where the inflaton field gradually rolls toward the minimum of its potential. This straightforward single-field inflation model assumes the cosmological principle, implying a homogeneous and isotropic background geometry.

On the other hand, when we physically describe the very early moments in the history of the universe, it may not be enough to just consider a simple isotropic geometry. Also, from recent observational data, it is revealed that there are some anomalies in the cosmic microwave background radiation [5]. Some cosmologists believe that these anomalies have instrumental origins [6]. Also, the authors of [7] suggest that some observed anomalies in the Cosmic Microwave Background (CMB) may result from systematic effects such as asymmetric beams. While, some other cosmologists relate these anomalies to a homogeneous but anisotropic universe [8]. In this regard, Ref. [9] investigates how inflationary perturbations in anisotropic backgrounds affect the CMB and how data can be used to identify these effects. Ref. [10] also investigates the predictions from an anisotropic inflationary era and its effects on various cosmological features. There are various confrontations to the anisotropy. According to the prediction of the cosmic no-hair conjecture, the universe eventually approaches a homogeneous and isotropic state, even if it started from an anisotropic state [11]. In Ref. [12], the local validity of this conjecture has been proved. In paper [13] it has been shown that the power-law inflation acts as a local attractor for inhomogeneous solutions in a model with a minimally coupled scalar field and a positive exponential potential. In Ref. [14] the role of initial conditions in inflationary cosmology and challenges the cosmic "no-hair" conjecture have been examined. Exact solutions of Einstein's equations in a case with an inhomogeneous scalar field, resulting in an intrinsically inhomogeneous metric have been studied in Ref. [15]. However, the authors of Ref. [16] have explored the possibility of anisotropy in the late-time universe. In Ref. [17], one can find a comprehensive review of FLRW anomalies. Some counterexamples questioning the validity of the no-hair conjecture can also be found in Ref. [18]. Also, the authors of [19] have explored Bianchi I and II universes in quadratic gravity, finding early-time isotropization and new anisotropic inflationary behaviors. Paper [20] presents new anisotropic solutions in higher-order gravity theories, exploring Bianchi type VIII, IX, and I cosmologies near the initial singularity and their relevance to cosmic "no-hair" theorems. The authors of [21] have studied the past evolution of an anisotropic Bianchi I universe in $f(R)$ gravity. Of course, according to the studies in Ref. [22], it seems that some of these counterexamples are unstable during the inflationary phase of the universe. Also, in Ref. [23] it has been found that anisotropic solutions in a conformal-violating Maxwell model are unstable during inflation but can persist in a slowly expanding phase for certain parameters. The authors of Ref. [24] proved an inflationary cosmic no-hair theorem, which allows for a certain level of anisotropy. In the supergravity-based model also, a counterexample to the conjecture has been found which seems interesting [25].

Therefore, by considering the fact that anisotropy may have an important role in the history of the universe, some cosmologists have performed interesting works on this issue. By incorporating additional quadratic Ricci curvature terms into the Einstein-Hilbert action, Ref. [26] explores several cosmological solutions. The power spectrum in anisotropic inflation has been examined in Ref. [27], where a specific coupling between the gauge field and the inflaton was considered by the authors. Ref. [28] presents exact solutions for anisotropic power-law inflation, achieved by introducing exponential potentials for the inflaton and the gauge field. Another interesting case has been studied in Ref. [29]. The study demonstrates anisotropic power-law inflation, relying on exponential forms for the inflaton potential. One can find the cosmological aspects of anisotropic constant-roll inflation in Ref. [30]. The properties of scalar and tensor perturbations in the non-canonical anisotropic inflation have been studied in Ref. [31]. The authors of Ref. [32] derived an anisotropic power-law solution by introducing two scalar fields which are non-minimally coupled to two vector fields. A hyperbolic inflation model along a gauge field has been considered in Ref. [33], where the authors have explored anisotropic inflation. Based on the Bianchi IX cosmology, the authors of Ref. [34] have considered the general form of the metric and examined the anisotropic inflation in the cosmological models with $F(R)$ gravity. Thus, it seems interesting to consider anisotropic property in the cosmological model and study its cosmological implication. In fact, the presence of the anisotropic geometry may affect the cosmological viability of the models. Particularly when the slow-roll parameters are influenced by anisotropic effects, it would affect for instance the scalar spectral index and the tensor-to-scalar ratio. By comparing the numerical values of these parameters with observational data it is possible to find some constraints on the anisotropic parameter. Also, we can explore the presence of anisotropic geometry in the reheating phase after inflation to find some extra information.

Now, in this paper, we consider single-field model with intermediate scale factor in the anisotropic background and revisit the inflation in this setup. Usually, anisotropic aspects seem less relevant in the canonical scalar field model for inflation. This is because the exponential expansion quickly dilutes any initial anisotropy. However, here we focus on an intermediate inflation model. Unlike standard exponential inflation, the intermediate model features a slower expansion rate, which might allow some anisotropy to persist. Our goal is to how it impacts the model's viability. By using the slow-roll, perturbations and reheating parameters, we try to check this anisotropic model observationally. The structure of the paper is as follows. In section 2, we study the anisotropic inflation and find some important equations and parameters in this setup. In section 3, we explore the observational viability of the intermediate anisotropic inflation in comparison with the observational data. The reheating phase after inflation is considered in 4. In section 5, we present a summary of the model.

2 Anisotropic Inflation

To revisit the anisotropic inflation, we consider a homogeneous but anisotropic background geometry defined by the following metric [34]

$$ds^2 = -dt^2 + a(t)^2 \sum_{i=1}^3 e^{2\xi_i(t)} (dx^i)^2. \quad (1)$$

In this metric, we defined

$$\bar{\xi}(t) = \frac{1}{3} \sum_{i=1}^3 \xi_i(t), \quad (2)$$

which gives the the average value of the parameter $\xi_i(t)$. Following Ref. [34], it is possible to express

$$a(t) \rightarrow a(t) + \bar{\xi}(t) \quad (3)$$

and

$$\xi_i(t) \rightarrow \xi_i(t) - \bar{\xi}(t). \quad (4)$$

In this way, we find

$$\sum_{i=1}^3 \xi^i = 0 \quad (5)$$

and

$$\sum_{i=1}^3 \dot{\xi}^i = 0. \quad (6)$$

Therefore, we can find the components of the Ricci tensor as [35]

$$\mathcal{R}_{00} = - \sum_{i=1}^3 (\dot{\xi}^i)^2 - 3\dot{H} - 3H^2, \quad (7)$$

$$\mathcal{R}_{ij} = \left(\dot{H} + 3H^2 + \ddot{\xi}^i + 3H\dot{\xi}^i \right) a^2 e^{2\xi_i} \delta_{ij}. \quad (8)$$

Note that, in the equations of this paper, we use a dot to demonstrate a cosmic time. We also find the Ricci scalar in the anisotropic background as [35]

$$\mathcal{R} = \sum_{i=1}^3 (\dot{\xi}^i)^2 + 6\dot{H} + 12H^2. \quad (9)$$

In studying the inflation phase in every model, the Friedmann equations play an important and critical role. To obtain these equations in the anisotropic geometry situation, we use (0,0) and (i,i) components of the Einstein field equations and find

$$H^2 = \frac{\kappa^2}{3} \left(\frac{1}{2} \dot{\phi}^2 + V(\phi) \right) + \frac{1}{6} \sum_{i=1}^3 (\dot{\xi}^i)^2, \quad (10)$$

$$2\dot{H} + 3H^2 = -\kappa^2 \left(\frac{1}{2} \dot{\phi}^2 - V(\phi) \right) - \frac{1}{2} \sum_{i=1}^3 (\dot{\xi}^i)^2, \quad (11)$$

where, $\kappa^2 = 8\pi G$ is the gravitational constant. Also, to obtain these equation, we have used equations (7)-(9). By checking the equation of motion, we see that the anisotropic doesn't have any effect on it and we reach the usual formulae as

$$\ddot{\phi} + 3H\dot{\phi} + V' = 0. \quad (12)$$

From now on, we use a prime to show $\frac{d}{d\phi}$.

By considering the Friedmann equations, the potential in this model is obtained as

$$V = \frac{6H^2 - \kappa^2 \dot{\phi}^2 - \sum_{i=1}^3 (\dot{\xi}^i)^2}{2\kappa^2}, \quad (13)$$

with

$$\dot{\phi} = \frac{\sqrt{-2\dot{H} - \sum_{i=1}^3 (\dot{\xi}^i)^2}}{\kappa}. \quad (14)$$

At this point, from the definition of the slow-roll parameters as $\epsilon = -\frac{\dot{H}}{H^2}$ and $\eta = \frac{1}{H} \dot{\epsilon}$, and by using equations (10)-(13), we find these parameters in the anisotropic inflation model as

$$\epsilon = \frac{1}{2\kappa^2} \frac{V'^2}{V^2} + \frac{3 \sum_{i=1}^3 (\dot{\xi}^i)^2}{\kappa^2 V + \frac{1}{2} \sum_{i=1}^3 (\dot{\xi}^i)^2}, \quad (15)$$

$$\eta = -\frac{2}{\kappa^2} \frac{V''}{V} + \frac{2}{\kappa^2} \frac{V'^2}{V^2} - \frac{9}{2\kappa^2} \frac{\sqrt{\frac{\kappa^2}{3} V + \frac{1}{6} \sum_{i=1}^3 (\dot{\xi}^i)^2} \frac{d}{dt} \sum_{i=1}^3 (\dot{\xi}^i)^2}{V'^2} + \frac{6 \sum_{i=1}^3 (\dot{\xi}^i)^2}{\kappa^2 V + \frac{1}{2} \sum_{i=1}^3 (\dot{\xi}^i)^2}. \quad (16)$$

To have inflationary era, these slow-roll parameters must be very smaller than unity and when one of them becomes unit at some point of time, the inflation ends. In the cosmological models, duration of the inflation is given by e-folds number (N), defined as

$$N = \int_{t_i}^{t_f} H dt, \quad (17)$$

with i and f denoting the beginning and end of this era. Now, by using the perturbation parameters defined as [36]

$$n_s - 1 = -2\epsilon - \eta, \quad (18)$$

and

$$r = 16\epsilon, \quad (19)$$

We can examine how the anisotropic geometry influences the observational viability of the model. In the next section, we numerically analyze the model using an intermediate scale factor and compare the results with observational data.

3 Observational Viability of the Model

To study the model numerically, we must find some explicit expressions for the perturbation parameters. In this regard, we first find some expression for $\dot{\xi}$ that appears in all our equations. To this end, we follow Ref. [34], where it has been shown that the parameter ξ satisfies the following equation

$$\ddot{\xi}^i + 3H \dot{\xi}^i = 0. \quad (20)$$

Its solution gives $\dot{\xi}^i$ as a function of time as

$$\dot{\xi}^i = \frac{C^i}{a^3}, \quad (21)$$

with C^i 's to be some constants. Equation (21), along with $\Sigma_{i=1}^3 \dot{\xi}^i = 0$, leads to the constraint $\Sigma_{i=1}^3 C^i = 0$. These equations are very important in the numerical study of the setup. To proceed, we adopt the intermediate scale factor defined by (see for instance [37])

$$a = a_0 \exp(bt^\beta), \quad (22)$$

with b to be a constant and also $0 < \beta < 1$. By using this equation, we can find H and its derivatives in terms of the time. Then, by using the definition of the e-folds number we obtain the time in terms of N . In this way, all equations which include a or H or their derivatives, become function of N . This means that we can write $H = N \left(\frac{N}{b}\right)^{-\frac{1}{\beta}} \beta$ and $\dot{\xi} = \frac{C^i}{a_0^3 e^{3N}}$. Then, we substitute these definitions in equations (13), (15) and (16), and find the slow-roll parameters in this setup as

$$\begin{aligned} \epsilon = & \frac{\left(\frac{6\beta^2 b^2 (\chi^{\beta-1})^2 (\beta-1)}{\chi} + \frac{\beta b \chi^{\beta-1} (\beta-1)^2}{\chi^2} - \frac{\beta b \chi^{\beta-1} (\beta-1)}{\chi^2}\right)^2}{2 \left(-\frac{2\beta b \chi^{\beta-1} (\beta-1)}{\chi} - \frac{c^2}{(a_0)^6 (e^b \chi^\beta)^6}\right) \left(3\beta^2 b^2 (\chi^{\beta-1})^2 + \frac{\beta b \chi^{\beta-1} (\beta-1)}{\chi}\right)^2} \\ & + \frac{3c^2}{(a_0)^6 (e^b \chi^\beta)^6 \left(3\beta^2 b^2 (\chi^{\beta-1})^2 + \frac{\beta b \chi^{\beta-1} (\beta-1)}{\chi} + \frac{c^2}{2(a_0)^6 (e^b \chi^\beta)^6}\right)}, \quad (23) \end{aligned}$$

and

$$\begin{aligned} \eta = & \frac{2}{3\beta^2 b^2 (\chi^{\beta-1})^2 + \frac{Y}{\chi}} \left(\frac{\kappa \left(-\frac{2Y(\beta-1)}{\chi^2} + \frac{2Y}{\chi^2} + \frac{6c^2 b \chi^\beta \beta}{(a_0)^6 (e^b \chi^\beta)^6 \chi}\right) \left(\frac{6\beta b \chi^{\beta-1} Y}{\chi} + \frac{Y(\beta-1)}{\chi^2} - \frac{Y}{\chi^2}\right)}{2 \left(-\frac{2Y}{\chi} - \frac{c^2}{(a_0)^6 (e^b \chi^\beta)^6}\right)^{\frac{5}{2}}} \right. \\ & \left. + \frac{\frac{6Y^2}{\chi^2} + 6\beta b \chi^{\beta-1} \left(\frac{Y(\beta-1)}{\chi^2} - \frac{Y}{\chi^2}\right) + \frac{Y(\beta-1)^2}{\chi^3} - \frac{3Y(\beta-1)}{\chi^3} + \frac{2Y}{\chi^3}}{\frac{2Y}{\chi} + \frac{c^2}{(a_0)^6 (e^b \chi^\beta)^6}} \right) \\ & + \frac{2 \left(\frac{6\beta b \chi^{\beta-1} Y}{\chi} + \frac{Y(\beta-1)}{\chi^2} - \frac{Y}{\chi^2}\right)^2}{\left(\frac{2Y}{\chi} + \frac{c^2}{(a_0)^6 (e^b \chi^\beta)^6}\right) \left(3\beta^2 b^2 (\chi^{\beta-1})^2 + \frac{Y}{\chi}\right)^2} + \frac{c^2 b \chi^\beta \beta \left(-\frac{2Y}{\chi} - \frac{c^2}{(a_0)^6 (e^b \chi^\beta)^6}\right)}{2(a_0)^6 (e^b \chi^\beta)^6 \chi \left(\frac{6\beta b \chi^{\beta-1} Y}{\chi} + \frac{Y(\beta-1)}{\chi^2} - \frac{Y}{\chi^2}\right)^2} \\ & \times 9 \sqrt{36\beta^2 b^2 (\chi^{\beta-1})^2 + \frac{12Y}{\chi} + \frac{6c^2}{(a_0)^6 (e^b \chi^\beta)^6}} \\ & + \frac{6c^2}{(a_0)^6 (e^b \chi^\beta)^6 \left(3\beta^2 b^2 (\chi^{\beta-1})^2 + \frac{\beta b \chi^{\beta-1} (\beta-1)}{\chi} + \frac{c^2}{2(a_0)^6 (e^b \chi^\beta)^6}\right)}, \quad (24) \end{aligned}$$

Table 1: Ranges of the parameter c in which the tensor-to-scalar ratio and scalar spectral index of the intermediate anisotropic model are consistent with different data sets.

β	Planck2018 TT,TE,EE+lowE +lensing+BK14+BAO	Planck2018 TT,TE,EE+lowE +lensing+BK14+BAO	Planck2018 TT,TE,EE+lowE lensing+BK18+BAO	Planck2018 TT,TE,EE+lowE lensing+BK18+BAO
	68% CL	95% CL	68% CL	95% CL
0.8	not consistent	$7.67 < c < 8.15$	not consistent	not consistent
0.85	$7.45 < c < 7.74$	$7.21 < c < 7.97$	not consistent	not consistent
0.9	$7.47 < c < 8.05$	$7.27 < c < 8.30$	not consistent	$7.45 < c < 8.23$
0.95	$8.83 < c < 9.69$	$8.58 < c < 10.02$	$8.87 < c < 9.78$	$8.63 < c < 10.09$

where,

$$\chi = \left(\frac{N}{b}\right)^{\frac{1}{\beta}}, \quad Y = \beta b \chi^{\beta-1} (\beta - 1), \quad c^2 = \sum_{i=1}^3 C^{i^2}. \quad (25)$$

We substitute equations (23) and (24), in the definitions of the scalar spectral index (18) and tensor-to-scalar ratio (19), to perform some numerical analysis on the model. In our analysis, we use the values of the scalar spectral index and tensor-to-scalar ratio, released by Planck2018 TT, TE, EE +lowE+lensing+BK14+BAO data and based on Λ CDM+ $r+\frac{dn_s}{d\ln k}$ model, as $n_s = 0.9658 \pm 0.0038$ and $r < 0.072$ [38]. Also, we consider another constraint on the tensor-to-scalar ratio as $r < 0.036$, obtained from Planck2018 TT, TE, EE +lowE+lensing+BK18+BAO data [39]. In this way, in figure 1, we show the evolution of $r - n_s$ in comparison with Planck2018 TT, TE, EE +lowE+lensing+BK14(18)+BAO data. To plot this figure, we have considered $7 < c < 30$ and $0.7 < \beta < 1$. In this way, we have found constraints on c using sample values of β . These constraints are summarized in table 1. According to our analysis, the model is consistent with Planck2018 TT, TE, EE +lowE+lensing+BK14(18)+BAO data at 68% CL if $0.84 < \beta < 1$ and $7.70 < c < 27.3$ ($0.91 < \beta < 1$ and $8.03 < c < 27.2$)⁴. The model is consistent with the mentioned data at 95% CL if $0.77 < \beta < 1$ and $8.40 < c < 28.5$ ($0.88 < \beta < 1$ and $7.64 < c < 28.5$). The phase space of the anisotropic parameter c and intermediate parameter β , corresponding to the 68% CL and 95% CL of Planck2018 TT, TE, EE +lowE+lensing+BK14(18)+BAO constraints on n_s and r , is shown in figure 2. Note that, in plotting the figures, we have adopted $N = 60$ and $b = 1$. According to our analysis, the intermediate anisotropic inflation in some ranges of its model's parameters is consistent with recent observational data. We also can check the viability of the model from different perspectives. One interesting perspective is the study of the reheating phase of the universe in this model. In the following, we try to explore the model within this context and find some more constraints on the model's main parameters.

⁴The constraints in the parentheses have been obtained from Planck2018 TT, TE, EE +lowE +lensing +BK18 +BAO data.

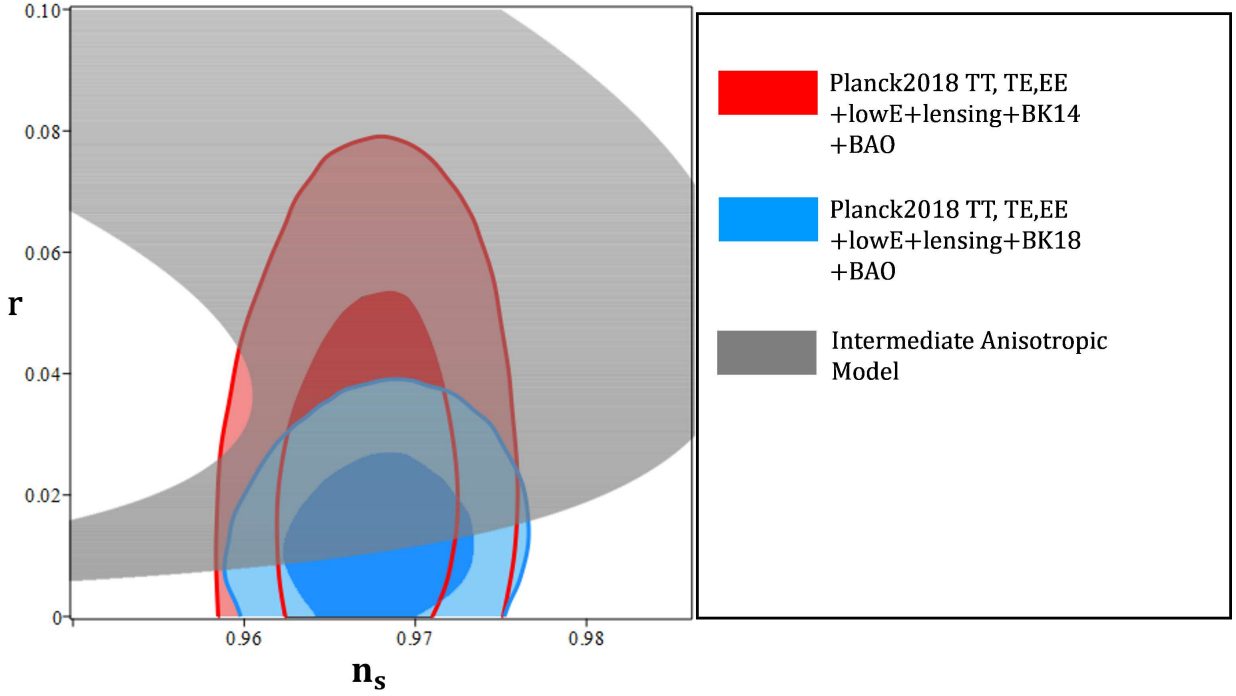


Figure 1: $r - n_s$ behavior for the anisotropic inflationary model with intermediate scale factor, in the background of Planck2018 TT, TE, EE +lowE+lensing+BK14(18) +BAO data. The varying parameters in this figure are c and β .

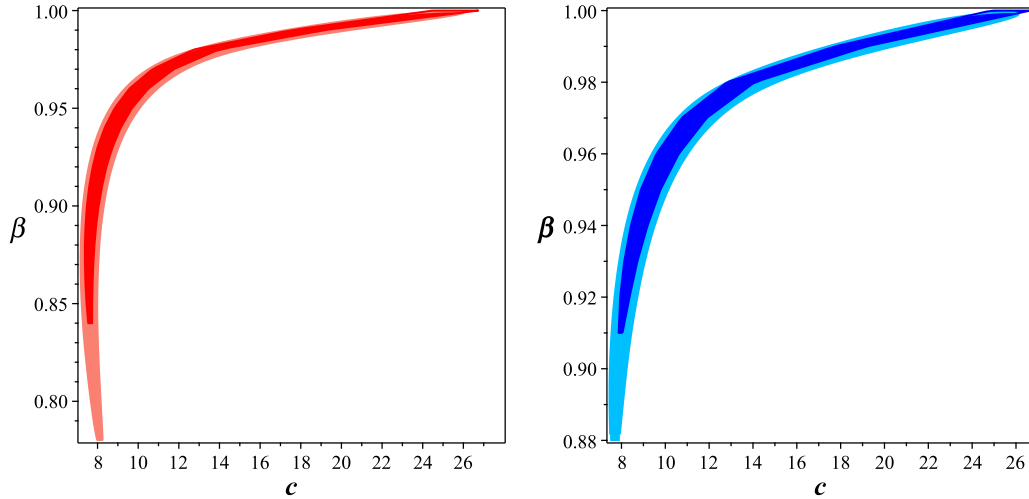


Figure 2: The phase space of the intermediate parameter β and anisotropic parameter c , corresponding to the Planck2018 TT, TE, EE +lowE+lensing+BK14+BAO data (left panel) and Planck2018 TT, TE, EE +lowE+lensing+BK18+BAO data (right panel) at 68% CL (deep colors) and 95% CL (light colors). This figure has been plotted based on the observational constraints on the scalar spectral index and tensor-to-scalar ratio.

4 Reheating

After the end of the early inflationary phase of the universe, the temperature of the universe becomes very low. Therefore the universe couldn't be prepared to be governed by the standard model of cosmology. It seems that, considering a reheating phase after the end of inflation can solve this issue properly. In this regard, in [40] it has been shown that the canonical reheating is possible in ϕ^2 potential. The authors of Ref. [41] have constrained the equation of state parameters during the reheating. In this paper, we use the strategy considered in the mentioned papers and also Res. [42] to examine the reheating process in this setup (for other strategies see for instance [43]). The details of this strategy can be seen in Appendix. In this regard, we can re-write the energy density in this setup as

$$\rho = \frac{\left(V + \frac{1}{2\kappa^2} \sum_{i=1}^3 (\dot{\xi}^i)^2\right)}{3} \left[\epsilon - \frac{3 \sum_{i=1}^3 (\dot{\xi}^i)^2}{\kappa^2 V + \frac{1}{2} \sum_{i=1}^3 (\dot{\xi}^i)^2} \right] + V. \quad (26)$$

To obtain this equation, we have used the equation of motion (12) and obtained $\dot{\phi}$ in terms of the potential and its derivative. Then, we have used equation (16) and found the V' in terms of the slow-roll parameter ϵ . After that we substitute these in the energy density of the scalar field ($\rho = \frac{1}{2}\dot{\phi}^2 + V(\phi)$) and reach the above equation for energy density. When we take $\epsilon = 1$, equation (26) gives us the energy density at the end of inflation as

$$\rho_e = \frac{\left(V_e + \frac{1}{2\kappa^2} \sum_{i=1}^3 (\dot{\xi}^i)^2\right)}{3} \left[1 - \frac{3 \sum_{i=1}^3 (\dot{\xi}^i)^2}{\kappa^2 V_e + \frac{1}{2} \sum_{i=1}^3 (\dot{\xi}^i)^2} \right] + V_e. \quad (27)$$

leading to

$$\rho_{rh} = \left[\frac{\left(V_e + \frac{1}{2\kappa^2} \sum_{i=1}^3 (\dot{\xi}^i)^2\right)}{3} \left(1 - \frac{3 \sum_{i=1}^3 (\dot{\xi}^i)^2}{\kappa^2 V_e + \frac{1}{2} \sum_{i=1}^3 (\dot{\xi}^i)^2} \right) + V_e \right] \exp \left[-3N_{rh}(1 + \omega_{eff}) \right]. \quad (28)$$

Now, with equation (28) we can write

$$\begin{aligned} \ln \left(\frac{a_0}{a_{rh}} \right) &= -\frac{1}{3} \ln \left(\frac{43}{11g_{rh}} \right) - \frac{1}{4} \ln \left(\frac{\pi^2 g_{rh}}{30} \right) - \ln T_0 - \frac{3}{4} N_{rh}(1 + \omega_{eff}) \\ &+ \frac{1}{4} \ln \left(\frac{\left(V_e + \frac{1}{2\kappa^2} \sum_{i=1}^3 (\dot{\xi}^i)^2\right)}{3} \left[1 - \frac{3 \sum_{i=1}^3 (\dot{\xi}^i)^2}{\kappa^2 V_e + \frac{1}{2} \sum_{i=1}^3 (\dot{\xi}^i)^2} \right] + V_e \right). \end{aligned} \quad (29)$$

With this equation, we can find the number of e-folds during the reheating in terms of the anisotropic and other model's parameters as

$$\begin{aligned} N_{rh} &= \frac{4}{1 - 3\omega_{eff}} \left[-N - \ln \left(\frac{k_{hc}}{a_0 T_0} \left(\frac{30}{\pi^2 g_{rh}} \right)^{\frac{1}{4}} \left(\frac{11g_{rh}}{43} \right)^{\frac{1}{3}} \right) + \frac{1}{2} \ln(H^2) \right. \\ &\left. - \frac{1}{4} \ln \left(\frac{\left(V_e + \frac{1}{2\kappa^2} \sum_{i=1}^3 (\dot{\xi}^i)^2\right)}{3} \left(1 - \frac{3 \sum_{i=1}^3 (\dot{\xi}^i)^2}{\kappa^2 V_e + \frac{1}{2} \sum_{i=1}^3 (\dot{\xi}^i)^2} \right) + V_e \right) \right], \end{aligned} \quad (30)$$

leading to the following expression for the reheating temperature

$$T_{rh} = \left(\frac{30}{\pi^2 g_{rh}} \right)^{\frac{1}{4}} \left[\frac{\left(V_e + \frac{1}{2\kappa^2} \sum_{i=1}^3 (\dot{\xi}^i)^2 \right)}{3} \left(1 - \frac{3 \sum_{i=1}^3 (\dot{\xi}^i)^2}{\kappa^2 V_e + \frac{1}{2} \sum_{i=1}^3 (\dot{\xi}^i)^2} \right) + V_e \right]^{\frac{1}{4}} \exp \left[-\frac{3}{4} N_{rh} (1 + \omega_{eff}) \right]. \quad (31)$$

Now, we have enough tools to explore the observational viability of the model in the context of the reheating process and by using the important parameters N_{rh} and T_{rh} . There are some points that should be taken care to be ready for numerical analysis. In equations (30) and (31), we see the parameter V_e . We can use the fact that at the end of inflation, we have $\epsilon = 1$. From this condition and equation (23), we find the parameter c in terms of other parameters (this gives us a very long-expression and we avoid presenting it here). Then, we substitute it in equation (13) to find the value of the potential at the end of the inflation. Note that, to find the full expression in terms of the model's constant parameters, we should use equations (21) and (22) too. Since we want to study the reheating parameter in comparison with observational data, we should have them in terms of some parameters that are constrained with data. We can write H^2 in the equation (30) in terms of the scalar spectral index. To this end, we consider the definition of the first slow-roll parameter as $\epsilon = -\frac{\dot{H}}{H^2}$. Then, we find $H^2 = -\epsilon \dot{H}$, where $\dot{H} = N^{\frac{\beta-2}{\beta}} \beta b^{\frac{2}{\beta}} (\beta - 1)$ in the intermediate model with $a = a_0 \exp(bt^\beta)$. On the other hand, we have $n_s = 1 - 2\epsilon - \eta$, leading to $\epsilon = \frac{1}{2}(1 - n_s - \eta)$. By substituting this recent equation in $H^2 = -\epsilon \dot{H}$, we find

$$H^2 = -\frac{1}{2} [1 - n_s - \eta] \left[N^{\frac{\beta-2}{\beta}} \beta b^{\frac{2}{\beta}} (\beta - 1) \right], \quad (32)$$

where η is given by equation (24). In this way, we obtain equations (30) and therefore (31) in terms of the scalar spectral index and perform some numerical analysis. We use the observational value of the scalar spectral index, $n_s = 0.9658 \pm 0.0038$, obtained from Planck2018 TT, TE, EE +lowE+lensing+BK14+BAO data. We also set $g_{rh} = 106.75$ [44] and $k_{hc} = 0.002 Mpc^{-1}$ as pivot scale [38]. By using these values, we obtain the observationally viable ranges of N_{rh} and ω_{eff} and results are shown in figure 3. In this figure, we have chosen two values for the intermediate and anisotropic parameters as $\beta = 0.85$, $c = 7.6$ and $\beta = 0.95$, $c = 9.5$. From the figure, it seems that for $\beta = 0.85$, $c = 8$ it is possible to have instantaneous reheating. However, for $\beta = 0.95$, $c = 9$, the universe reheats after a few numbers of e-folds. Since at the end of inflation era, the value of the effective equation of state is $-\frac{1}{3}$ and at the beginning of the radiation dominated era it is $\frac{1}{3}$, it is important for the model to cover this transition. According to the figure 3, it seems that by increasing the e-folds number during the reheating, the effective equation of state parameter increases from -1 to $\frac{1}{3}$ where the universe becomes radiation dominated. We have also plotted $N_{rh} - n_s$ and $T_{rh} - n_s$ behaviors for these sample values and for $\omega = -1$, $\omega = -\frac{1}{3}$ and $\omega = 0$ that have been shown in figures 4 and 5. By considering the observationally viable ranges of the anisotropic parameter, based on the observational constraints on n_s and r , we have obtained some constraints on the amount of the e-folds number and temperature, needed for the universe to be reheated. The results are shown in tables 2 and 3. The results are in both 68% CL and 95% CL. These data also show that in some regions of the model's parameters, it is possible to have instantaneous reheating phase. However, for some other regions, some e-folds needed in the reheating process. According to our analysis and in the ranges of the considered anisotropic and intermediate parameters, it seems that for $\omega = -1$, depending on the values of β and c , the constraint on the e-folds number and

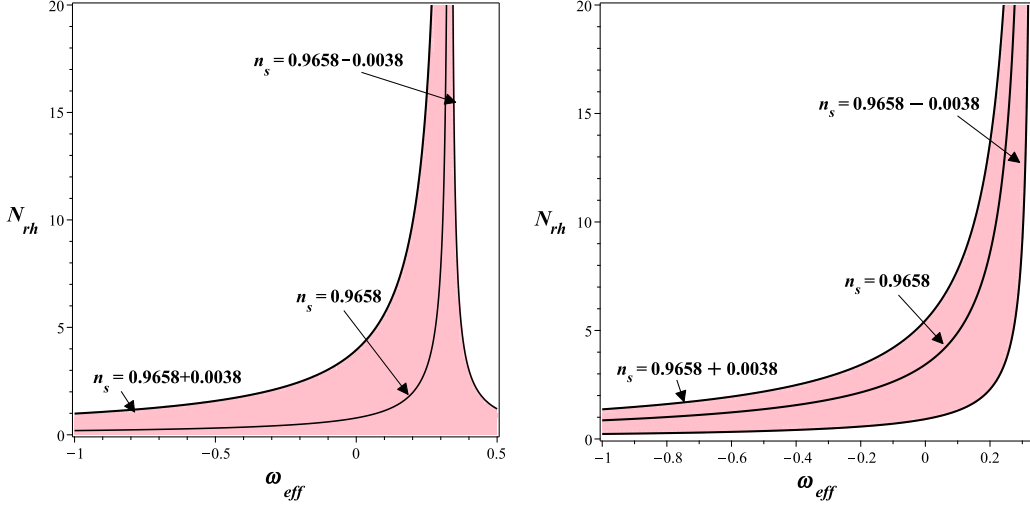


Figure 3: The observationally viable region of N_{rh} and ω_{eff} , based on the constraint on the scalar spectral index, obtained from the Planck2018 TT, TE, EE +lowE+lensing+BK14+BAO data. Not that, we have adopted $\beta = 0.85$ and $c = 7.6$ for the left panel, and $\beta = 0.95$ and $c = 9.5$ for the right panel.

temperature during reheating are respectively as $0 \leq N_{rh} \leq 1.80$ and $14.97 \leq \log_{10} \left(\frac{T_{rh}}{GeV} \right) \leq 15$ at 68% CL, and $0 \leq N_{rh} \leq 2.15$ and $14.96 \leq \log_{10} \left(\frac{T_{rh}}{GeV} \right) \leq 15$ at 95% CL. These constraints for $\omega = -\frac{1}{3}$ are as $0 \leq N_{rh} \leq 2.70$ and $-1.92 \leq \log_{10} \left(\frac{T_{rh}}{GeV} \right) \leq 15$ at 68% CL, and $0 \leq N_{rh} \leq 3.50$ and $-1.71 \leq \log_{10} \left(\frac{T_{rh}}{GeV} \right) \leq 15$ at 95% CL. Also, for $\omega = 0$ we have $0 \leq N_{rh} \leq 5.85$ and $-1.89 \leq \log_{10} \left(\frac{T_{rh}}{GeV} \right) \leq 15$ at 68% CL, and $0 \leq N_{rh} \leq 6.13$ and $-1.90 \leq \log_{10} \left(\frac{T_{rh}}{GeV} \right) \leq 15$ at 95% CL.

5 Conclusion

In this paper, we revisit intermediate inflation within an anisotropic geometry. By incorporating the Friedmann equations expressed in terms of anisotropic parameters, we derive the slow-roll parameters for this framework. Since the anisotropic property appears directly in the Friedmann equations, its effects appear in the slow-roll parameters too. This, consequently, affects the perturbations parameters scalar spectral index and tensor-to-scalar ratio. Then, in order to check the viability of the model, we have adopted the intermediate scale factor as $a = a_0 \exp(bt^\beta)$. We have also considered the anisotropic parameter $\xi^i = \frac{C^i}{a^3}$. By these choices, we have obtained the slow-roll parameters and therefore, the perturbations parameters in terms of the intermediate (β) and anisotropic (c) parameters. In this way, we have tried to perform some numerical analysis and find some constraints on β and c . To this end, we have considered both Planck2018 TT, TE, EE+lowE+lensing+BK14+BAO and Planck2018 TT, TE, EE+lowE+lensing+BK18+BAO data. We have studied $r - n_s$ behavior in comparison to these data and found some constraints on the model's parameters. We have also plotted the $\beta - c$ phase space at both 68% CL and 95% CL. The constraints that we have obtained from our analysis are $0.84 < \beta < 1$ and $7.34 < c < 27.7$ ($0.91 < \beta < 1$ and $8.00 < c < 27.4$)

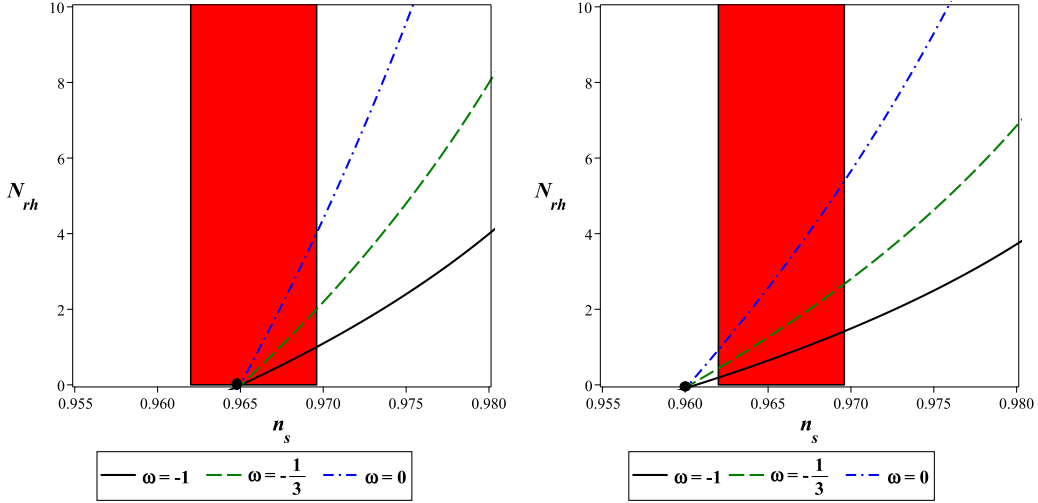


Figure 4: $N_{rh} - n_s$ behavior in the intermediate anisotropic model for some sample values as $\beta = 0.85$ and $c = 7.6$ (left panel), and $\beta = 0.95$ and $c = 9.5$ (right panel.)

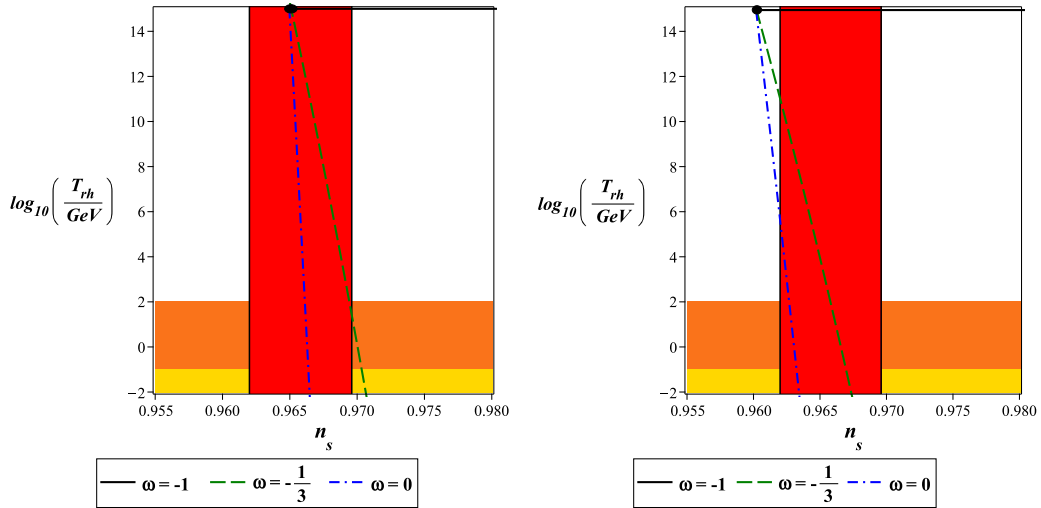


Figure 5: $\log_{10}\left(\frac{T_{rh}}{GeV}\right) - n_s$ behavior in the intermediate anisotropic model for some sample values as $\beta = 0.85$ and $c = 7.8$ (left panel), and $\beta = 0.95$ and $c = 9.8$ (right panel.) The orange region corresponds to the temperatures below the electroweak scale, $T < 100$ GeV, and the gold region stands for the temperatures below the big bang nucleosynthesis scale, $T < 10$ MeV.

Table 2: Constraints on N_{rh} in the anisotropic inflationary model with intermediate scale factor, based on the constraint on the scalar spectral index and tensor-to-scalar ratio, obtained from Planck2018 TT, TE, EE+lowE+lensing+BK14+BAO joint data at 68% CL and 95% CL.

	β	c	$\omega = -1$	$\omega = -\frac{1}{3}$	$\omega = 0$
68% CL	0.85	$7.45 < c < 7.74$	$0 \leq N_{rh} \leq 1.33$	$0 \leq N_{rh} \leq 2.27$	$0 \leq N_{rh} \leq 4.27$
	0.90	$7.47 < c < 8.05$	$0.04 \leq N_{rh} \leq 1.57$	$0.10 \leq N_{rh} \leq 2.43$	$0.72 \leq N_{rh} \leq 4.41$
	0.95	$8.83 < c < 9.69$	$0.10 \leq N_{rh} \leq 1.80$	$0.17 \leq N_{rh} \leq 2.70$	$0.78 \leq N_{rh} \leq 5.85$
95% CL	0.85	$7.21 < c < 7.97$	$0 \leq N_{rh} \leq 1.50$	$0 \leq N_{rh} \leq 2.35$	$0 \leq N_{rh} \leq 4.39$
	0.90	$7.27 < c < 8.30$	$0 \leq N_{rh} \leq 1.70$	$0.05 \leq N_{rh} \leq 2.53$	$0.64 \leq N_{rh} \leq 4.63$
	0.95	$8.58 < c < 10.02$	$0.08 \leq N_{rh} \leq 2.15$	$0.11 \leq N_{rh} \leq 3.50$	$0.74 \leq N_{rh} \leq 6.13$

Table 3: Constraints on the T_{rh} in the anisotropic inflationary model with intermediate scale factor, based on the constraint on the scalar spectral index and tensor-t-scalar ratio, obtained from Planck2018 TT, TE, EE+lowE+lensing+BK14+BAO joint data at 68% CL and 95% CL.

	β	c	$\omega = -1$	$\omega = -\frac{1}{3}$	$\omega = 0$
68% CL	0.85	$7.45 < c < 7.74$	$14.98 \leq \log_{10} \left(\frac{T_{rh}}{GeV} \right) \leq 15.00$	$1.14 \leq \log_{10} \left(\frac{T_{rh}}{GeV} \right) \leq 15$	$-1.90 \leq \log_{10} \left(\frac{T_{rh}}{GeV} \right) \leq 15$
	0.90	$7.47 < c < 8.05$	$14.98 \leq \log_{10} \left(\frac{T_{rh}}{GeV} \right) \leq 15.00$	$0.06 \leq \log_{10} \left(\frac{T_{rh}}{GeV} \right) \leq 14.37$	$-1.89 \leq \log_{10} \left(\frac{T_{rh}}{GeV} \right) \leq 8.87$
	0.95	$8.83 < c < 9.69$	$14.97 \leq \log_{10} \left(\frac{T_{rh}}{GeV} \right) \leq 14.99$	$-1.92 \leq \log_{10} \left(\frac{T_{rh}}{GeV} \right) \leq 9.89$	$-1.89 \leq \log_{10} \left(\frac{T_{rh}}{GeV} \right) \leq 3.14$
95% CL	0.85	$7.21 < c < 7.97$	$14.97 \leq \log_{10} \left(\frac{T_{rh}}{GeV} \right) \leq 15.00$	$1.02 \leq \log_{10} \left(\frac{T_{rh}}{GeV} \right) \leq 15$	$-1.91 \leq \log_{10} \left(\frac{T_{rh}}{GeV} \right) \leq 15$
	0.90	$7.27 < c < 8.30$	$14.96 \leq \log_{10} \left(\frac{T_{rh}}{GeV} \right) \leq 15.00$	$-1.80 \leq \log_{10} \left(\frac{T_{rh}}{GeV} \right) \leq 14.65$	$-1.90 \leq \log_{10} \left(\frac{T_{rh}}{GeV} \right) \leq 10.10$
	0.95	$8.58 < c < 10.02$	$14.96 \leq \log_{10} \left(\frac{T_{rh}}{GeV} \right) \leq 15.00$	$-1.71 \leq \log_{10} \left(\frac{T_{rh}}{GeV} \right) \leq 10.74$	$-1.90 \leq \log_{10} \left(\frac{T_{rh}}{GeV} \right) \leq 5.32$

based on Planck2018 TT, TE, EE +lowE+lensing+BK14(18)+BAO data at 68% CL. Also, we have obtained $0.77 < \beta < 1$ and $7.17 < c < 28.9$ ($0.88 < \beta < 1$ and $7.40 < c < 28.8$), based on Planck2018 TT, TE, EE +lowE+lensing+BK14(18)+BAO data at 95% CL. After that, we studied the reheating phase after inflation in the intermediate anisotropic model. We have obtained some important parameters such as the e-folds number and temperature parameters in terms of β and c . Then, we have used the observational constraints on β and c , to explore the viable ranges of the reheating parameters. In this regard, we have plotted the regions of N_{rh} and T_{rh} versus ω_{eff} that are observationally viable. We have shown that when we use the observationally viable ranges of the model's parameters, it is possible to have a viable reheating phase.

In summary, in the absence of the anisotropic effect, the intermediate inflation with a simple single scalar field is not consistent with new observational data. This point has been shown in figure 2, where the observationally viable ranges of c start from $c = 7$. Note that, this result holds even with $\beta = 1$, corresponding to pure exponential scale factor. In fact, the presence of the anisotropic leads to a shift in both the scalar spectral index and tensor-to-scalar ratio and makes them observationally viable. Therefore, it seems that the anisotropic geometry has an important role in the viability of the model. Also, the viable ranges of c and β is important in studying the reheating phase. As figure 3 shows, when the value of anisotropic parameter is larger, the instantaneous reheating is not possible (the right panel of figure 3). Also, for smaller values of c , the reheating process can happen instantaneously. In this regard, the value of c in the model seems important in the sense that it determines the type of reheating phase. With the obtained ranges of the anisotropic parameter, the model supports the big-bang nucleosynthesis. One important result in studying the reheating phase in our model is that by increasing the e-folds number during the reheating, the effective equation of state parameter increases from -1 to $\frac{1}{3}$ where the universe becomes radiation dominated.

ACKNOWLEDGMENTS

We thank the respected referees for the very insightful comments that have improved the quality of the paper considerably.

Appendix

Following Refs. [45], we consider the following relation for the e-folds number

$$N_{hc} = \ln \left(\frac{a_{end}}{a_{hc}} \right). \quad (33)$$

Note that this parameter is defined in the interval between the time when physical scales crosses the Hubble horizon (shown by hc) and the time when inflation ends (shown by end). In the next step, it is important to have the e-folds number during the reheating phase (N_{rh}) in terms of the effective equation of state (ω_{rh}) and energy density during the reheating. To do this, we can use $\rho \sim a^{-3(1+\omega_{eff})}$. Therefore, we obtain [45]

$$N_{rh} = \ln \left[\frac{a_{rh}}{a_{end}} \right] = -\frac{1}{3(1+\omega_{eff})} \ln \left[\frac{\rho_{rh}}{\rho_{end}} \right]. \quad (34)$$

We also have the following relation between the parameters at the time when the physical scales

cross the Hubble horizon

$$0 = \ln \left[\frac{k_{hc} H_{hc}^{-1}}{a_{hc}} \right], \quad (35)$$

leading to

$$N_{hc} + N_{rh} + \ln \left[\frac{k_{hc} H_{hc}^{-1}}{a_0} \right] + \ln \left[\frac{a_0}{a_{rh}} \right] = 0. \quad (36)$$

Now, we consider the following equation [45]

$$\rho_{rh} = \frac{\pi^2 g_{rh}}{30} T_{rh}^4, \quad (37)$$

which gives us the relation between the energy density and temperature during the reheating. In this equation, the parameter g_{rh} stands for the effective number of the relativistic species at the reheating phase. We have also the relation between the scale factor and temperature as [42, 45]

$$a_0 = \left(\frac{11 g_{rh} T_{rh}^3}{43 T_0^3} \right)^{\frac{1}{3}} a_{rh}. \quad (38)$$

Equations (37) and (38) give [45]

$$\frac{a_0}{a_{rh}} = \left(\frac{11 g_{rh}}{43 T_0^3} \right)^{\frac{1}{3}} \left(\frac{30 \rho_{rh}}{\pi^2 g_{rh}} \right)^{\frac{1}{4}}. \quad (39)$$

This is a useful equation in studying the reheating phase.

References

- [1] A. Guth, “Inflationary universe: A possible solution to the horizon and flatness problems”, *Phys. Rev. D* **23**, 347 (1981).
- [2] A. D. Linde, “A new inflationary universe scenario: A possible solution of the horizon, flatness, homogeneity, isotropy and primordial monopole problems”, *Physics Letters B* **108**, 389 (1982).
- [3] A. Albrecht & P. Steinhard, “Cosmology for Grand Unified Theories with Radiatively Induced Symmetry Breaking”, *Phys. Rev. D* **48**, 1220 (1982).
- [4] J. E. Lidsey, A. R. Liddle, E. W. Kolb, E. J. Copeland, T. Barreiro & M. Abney, “Reconstructing the inflaton potential an overview”, *Rev. Mod. Phys.* **69**, 373 (1997) [arXiv:astro-ph/9508078].
- [5] Y. Akrami, M. Ashdown, J. Aumont, C. Baccigalupi, M. Ballardini, et al., “Planck 2018 results. VII. Isotropy and Statistics of the CMB”, *A& A* **641**, A7 (2020) [arXiv:1906.02552 [astro-ph.CO]].

- [6] D. Hanson and A. Lewis, “Estimators for CMB statistical anisotropy”, *Phys. Rev. D* **80**, 063004 (2009) [arXiv:0908.0963 [astro-ph.CO]].
- [7] D. Hanson, A. Lewis and A. Challinor, “Asymmetric Beams and CMB Statistical Anisotropy”, *Phys. Rev. D* **81**, 103003 (2010) [arXiv:1003.0198 [astro-ph.CO]].
- [8] G. F. R. Ellis and M. A. H. MacCallum, “A class of homogeneous cosmological models”, *Commun. Math. Phys.* **12**, 108 (1969).
- [9] A. E. Gumrukcuoglu, C. R. Contaldi, and M. Peloso, “Inflationary perturbations in anisotropic backgrounds and their imprint on the cosmic microwave background”, *J. Cosmol. Astropart. Phys.* **07**, 005 (2007) [arXiv:0707.4179 [astro-ph]].
- [10] C. Pitrou, T. S. Pereira, and J. P. Uzan, “Predictions from an anisotropic inflationary era”, *J. Cosmol. Astropart. Phys.* **04**, 004 (2008) [arXiv:0801.3596 [astro-ph]].
- [11] G. W. Gibbons and S. W. Hawking, “Cosmological event horizons, thermodynamics, and particle creation”, *Phys. Rev. D* **15**, 2738 (1977).
- [12] A. A. Starobinsky, “Isotropization of arbitrary cosmological expansion given an effective cosmological constant”, *JETP Lett.* **37**, 66 (1983).
- [13] V. Muller, H. J. Schmidt, and A. A. Starobinsky, “Power-law inflation as an attractor solution for inhomogeneous cosmological models”, *Class. Quant. Grav.* **7**, 1163 (1990).
- [14] J. D. Barrow and J. Stein-Schabes, “The deflationary universe: An instability of the de Sitter universe”, *Phys. Lett. A* **103**, 315 (1984).
- [15] J. A. Stein-Schabes, “Inflation in spherically symmetric inhomogeneous models”, *Phys. Rev. D* **35**, 2345 (1987).
- [16] J. Colin, R. Mohayaee, M. Rameez, and S. Sarkar, “Evidence for anisotropy of cosmic acceleration”, *Astron. Astrophys.* **631**, L13 (2019) [arXiv:1808.04597 [astro-ph.CO]].
- [17] P. K. Aluri, P. Cea, P. Chingangbam, M.-C. Chu, R. G. Clowes, et. al., “Is the Observable Universe Consistent with the Cosmological Principle?”, *Class. Quant. Grav.* **40**, 094001 (2023) [arXiv:2207.05765 [astro-ph.CO]].
- [18] J. D. Barrow and S. Hervik, “Anisotropically inflating universes”, *Phys. Rev. D* **73**, 023007 (2006) [arXiv:gr-qc/0511127].
- [19] J. D. Barrow and S. Hervik, “Evolution of universes in quadratic theories of gravity”, *Phys. Rev. D* **74**, 124017 (2006) [arXiv:gr-qc/0610013].
- [20] J. Middleton, “On The Existence Of Anisotropic Cosmological Models In Higher-Order Theories Of Gravity”, *Class. Quant. Grav.* **27**, 225013 (2010) [arXiv:1007.4669 [gr-qc]].
- [21] D. Muller, A. Ricciardone, A. A. Starobinsky, and A. Toporensky, “Anisotropic cosmological solutions in $R + R^2$ gravity”, *Eur. Phys. J. C* **78**, 311 (2018) [arXiv:1710.08753 [gr-qc]].

- [22] W. F. Kao and I. C. Lin, “Stability of the anisotropically inflating Bianchi type VI expanding solutions”, *Phys. Rev. D* **83**, 063004 (2011).
- [23] T. Q. Do and W. F. Kao and I. C. Lin, “Anisotropic power-law inflation for a conformal-violating Maxwell model”, *J. Cosmol. Astropart. Phys.* **01**, 022 (2009) [arXiv:1712.03755 [gr-qc]].
- [24] A. Maleknejad and M. M. Sheikh-Jabbari, “Revisiting cosmic no-hair theorem for inflationary settings”, *Phys. Rev. D*, **85**, 123508 (2012) [arXiv:1203.0219 [hep-th]].
- [25] M. A. Watanabe, S. Kanno, and J. Soda, “Inflationary Universe with Anisotropic Hair”, *Phys. Rev. Lett.* **102**, 191302 (2009) [arXiv:0902.2833 [hep-th]].
- [26] J. D. Barrow and S. Hervik, “Simple types of anisotropic inflation”, *Phys. Rev. D* **81**, 023513 (2010) [arXiv:0911.3805 [gr-qc]].
- [27] T. R. Dulaney and M. I. Gresham, “Primordial power spectra from anisotropic inflation”, *Phys. Rev. D* **81**, 103532 (2010) [arXiv:1001.2301 [astro-ph.CO]].
- [28] S. Kanno, J. Soda, and M. a. Watanabe, “Anisotropic power-law inflation”, *J. Cosmol. Astropart. Phys.* **12**, 024 (2010) [arXiv:1010.5307 [hep-th]].
- [29] S. Lahiri, “Anisotropic inflation in Gauss-Bonnet gravity”, *J. Cosmol. Astropart. Phys.* **09**, 025 (2016) [arXiv:1605.09247 [hep-th]].
- [30] A. Ito and J. Soda, “Anisotropic constant-roll Inflation”, *Eur. Phys. J. C* **78**, 55 (2018) [arXiv:1710.09701 [hep-th]].
- [31] T. Q. Do, W. F. Kao and I.-C. Lin, “CMB imprints of non-canonical anisotropic inflation”, *Eur. Phys. J. C* **81**, 390 (2021) [arXiv:2003.04266 [gr-qc]].
- [32] T. Q. Do and W. F. Kao, “Anisotropic power-law inflation for a model of two scalar and two vector fields”, *Eur. Phys. J. C* **81**, 525 (2021) [arXiv:2104.14100 [gr-qc]].
- [33] C. -B. Chen and J. Soda, “Anisotropic hyperbolic inflation”, *J. Cosmol. Astropart. Phys.* **09**, 026 (2021) [arXiv:2106.04813 [hep-th]].
- [34] S. Nojiri, S .D. Odintsov, V. K. Oikonomou and A. Constantini, “Formalizing anisotropic inflation in modified gravity”, *Nuclear Physics B* **985**, 116011 (2022) [arXiv:2210.16383 [gr-qc]].
- [35] N. Rashidi, “Viable anisotropic inflation and reheating in the tachyon model”, *Eur. Phys. J. C* **84**, 99 (2024).
- [36] A. De Felice and S. Tsujikawa, “Primordial non-Gaussianities in general modified gravitational models of inflation”, *JCAP* **1104**, 029 (2011).
- [37] K. Nozari and N. Rashidi, “Mimetic DBI Inflation in Confrontation with Planck2018 Data”, *ApJ* **882**, 78 (2019).

- [38] Y. Akrami, F. Arroja, M. Ashdown, J. Aumont, C. Baccigalupi, et al., “Planck 2018 results. X. Constraints on inflation”, *A& A* **641**, A10 (2020) [arXiv:1807.06211 [astro-ph.CO]].
- [39] D. Paoletti, F. Finelli, J. Valiviita, M. Hazumi, “Planck and BICEP/Keck Array 2018 constraints on primordial gravitational waves and perspectives for future B -mode polarization measurements”, *Phys. Rev. D* **106**, 083528 (2022) [arXiv:2208.10482 [astro-ph.CO]].
- [40] L. Dai, M. Kamionkowski and J. Wang, “Reheating Constraints to Inflationary Models”, *Phys. Rev. Lett.* **113**, 041302 (2014) [arXiv:1404.6704 [astro-ph.CO]].
- [41] J. B. Munoz and M. Kamionkowski, “Equation of state parameter for reheating”, *Phys. Rev. D* **91**, 043521 (2015) [arXiv:1412.0656 [astro-ph.CO]].
- [42] J. L. Cook, E. Dimastrogiovanni, D. Easson and L. M. Krauss, “Reheating predictions in single field inflation”, *J. Cosmol. Astropart. Phys.* **04**, 047 (2015) [arXiv:1502.04673 [astro-ph.CO]].
- [43] M. Kawasaki, K. Kohri and N. Sugiyama, “MeV-scale reheating temperature and thermalization of the neutrino background”, *Phys. Rev. D* **62**, 023506 (2000) [arXiv:astro-ph/0002127].
- [44] Paolo Creminelli et al., “ ϕ^2 Inflation at its Endpoint”, *Phys. Rev. D* **90**, 083513 (2014).
- [45] Y. Ueno and K. Yamamoto, “Constraints on α -attractor inflation and reheating”, *Phys. Rev. D* **93**, 083524 (2016) [arXiv:1602.07427 [astro-ph.CO]].